

Original Research

# Artificial Neural Network Predictions of Up-Flow Anaerobic Sludge Blanket (UASB) Reactor Performance in the Treatment of Citrus Juice Wastewater

Moiz Elnekave<sup>1</sup>, Suna Ozden Celik<sup>2</sup>, Melkon Tatlier<sup>1</sup>, Nese Tufekci<sup>3\*</sup>

<sup>1</sup>Department of Chemical Engineering, Istanbul Technical University,  
34469, Maslak, Istanbul, Turkey

<sup>2</sup>Department of Environmental Engineering, Corlu Engineering Faculty, Namik Kemal University,  
59860, Corlu, Tekirdağ, Turkey

<sup>3</sup>Department of Environmental Engineering, Faculty of Engineering, Istanbul University,  
34320 Avcilar, Istanbul, Turkey

Received: 23 January 2011

Accepted: 27 May 2011

## Abstract

The operation of a full-scale up-flow anaerobic sludge blanket (UASB) reactor treating citrus juice wastewater was observed for two years. The average total chemical oxygen demand (COD) removal efficiency was determined to be equal to 79% and 77%, for the first and second years of operation for this reactor, respectively. The average volumetric loading rate was equal to 8.1 and 5.7 kg COD/m<sup>3</sup>day, respectively, during these periods. Three artificial neural network (ANN) models, namely feed forward back propagation (FFBP), radial basis function-based neural networks (RBF), and generalized regression neural networks (GRNN) were utilized to predict the COD and total suspended solid (TSS) concentrations in the effluent leaving the UASB reactor as well as the biogas production in the reactor. In general, the FFBP model made the best predictions with an average deviation of about 6.4-15.6% from the experimental values. The predictions made for biogas production and COD concentration were more accurate, while relatively larger discrepancies existed for the TSS concentration. The utilization of the ANN models generally provided significant improvements when compared to the use of multilinear regression for the same purpose.

**Keywords:** artificial neural network models, chemical oxygen demand, citrus juice wastewater, multilinear regression, UASB

## Introduction

The anaerobic process is a promising technology that presents advantages compared to the classical aerobic treatment: It has a high capacity for degrading concentrated waste, produces little sludge, and requires relatively less energy [1-3]. However, in spite of these advantages,

anaerobic treatment plants are still rare at the industrial scale, especially in developing countries, because they are known to become easily unstable under some circumstances, such as variations occurring in the process operating conditions and due to the requirement of a high level of expertise for operation. Nevertheless, these drawbacks can be overcome by associating feedback control for assuring a stable performance of the wastewater treatment operation.

---

\*e-mail: nese@istanbul.edu.tr

One of the most popular anaerobic treatment techniques is the up-flow anaerobic sludge blanket (UASB) process developed in the 1970s by Lettinga and co-workers in the Netherlands [4]. Application of the UASB process in the treatment of municipal and industrial wastewater was widely reported [5, 6]. Anaerobic digestion of cheese whey using the UASB reactor was also reported [7, 8].

There is a need to develop methodologies to determine UASB reactor performance, both for designing more efficient reactors and predicting the performance of the existing ones under various influent wastewater flow conditions. Based on qualitative understanding of the UASB process gained over the years, several attempts were made to develop mechanistic models for quantitative descriptions of UASB reactor performance [9-13].

Mechanistic models may remain insufficient due to several shortcomings in the available models. For example, the models might not be able to represent accurately the substrate availability to methanogenic microorganisms, i.e. the rate and extent of the formation and composition of volatile fatty acid in the reactor. The biochemical dynamics in the reactor have been simplified excessively, resulting in inaccurate depiction of the population and relative speciation of methanogenic microorganisms and their substrate utilization rates. Additionally, generally simplistic approaches have been used to explain the effects of biomass retention time, specific gas production rates of methanogens and sludge retention mechanisms on reactor performance. These and other deficiencies in mechanistic model formulation are primarily due to insufficient qualitative understanding of the process dynamics in the UASB reactor under various input conditions, and may only be overcome through additional empirical observation and analysis of experimental data on UASB reactor performance [14].

It may be useful to apply black-box models such as artificial neural networks to explain or predict the rather complex operation of a UASB reactor treating wastewater from industrial or domestic sources under different input conditions. A few studies have been performed related to the application of neural networks for the operation of UASB reactors. A neural network model was designed and trained to predict the steady-state performance of a UASB reactor treating high-strength (unrefined sugar-based) wastewater [14]. The model inputs were organic loading rate, hydraulic retention time, and influent bicarbonate alkalinity. The output variables were one or more of the effluent substrate concentration, reactor bicarbonate alkalinity, reactor pH, reactor volatile fatty acid concentration, average gas production rate, and percent methane content of the gas. The simulation results obtained were determined to provide insights into key variables that were responsible for influencing the working of the UASB reactor under varying input conditions. In another study, the steady-state performance of a granule-based  $H_2$ -producing UASB reactor was simulated using a hybrid neural network-genetic model [15]. Organic loading rate, hydraulic retention time (HRT) and influent bicarbonate alkalinity were the inputs of the model, whereas the output variables were one of the  $H_2$

concentration,  $H_2$  production rate,  $H_2$  yield, effluent total organic carbon, and effluent aqueous products, including acetate, propionate, butyrate, and valerate. The model described the daily variations of UASB reactor performance and predicted the steady-state reactor performance at various substrate concentrations and HRTs. In a different study, biogas production rate was modeled and estimated in a thermophilic UASB digester [16]. The data set covered a time period of both steady-state conditions and abnormal operation conditions, i.e. organic loading shocks. Multilayer neural network topology was used as the modeling tool and gave encouraging estimation results for the online control of thermophilic reactors.

In this study, the operation of an up-flow anaerobic sludge blanket (UASB) reactor treating citrus juice wastewater was observed for two years and then was modeled by three different artificial neural networks (ANNs). The predictability of the chemical oxygen demand (COD) and total suspended solid (TSS) concentrations in the effluent leaving the UASB reactor as well as the biogas production in the reactor was investigated. The results obtained were compared quantitatively to experimental values as well as to those determined by using multilinear regression.

## Material and Methods

### ANN Models Used

Artificial neural networks are black box models that can perform an estimation using limited input and output data patterns. They can model non-linear statistical data by simulating the structure and/or functional aspects of biological neural networks. In most cases, ANNs are adaptive systems that change structure depending on external or internal information that flows through the network during the learning phase. In this study, the feed forward back propagation (FFBP), generalized regression neural networks (GRNN), and radial basis function-based neural networks (RBF) models were used to relate some parameters in the UASB reactor to initial properties of the citrus juice influent.

Fig. 1 depicts the structure of FFBP neural networks. The FFBP configuration consists of an input layer, one or more hidden layers, and an output layer [17]. In a feed forward network, the input quantities are fed to the input nodes, which in turn pass them on to the hidden layer nodes after multiplying by weight. A hidden layer node, the function of which is to intervene between the external input and the network output, adds up the weighted input received from each input node, associates it with a bias, and then passes the result on to the nodes of the next hidden layer or the output, through a non-linear transfer function. The learning process works in small iterative steps. The output is compared to the known-good output, and a mean-squared error signal is calculated. The error value is then propagated backward through the network, and small changes are made to the weights in each layer. The weight changes are

calculated to reduce the error signal for the case in question. The cycle is repeated until the overall error value drops below some pre-determined threshold. The FFBP was trained using the Marquardt-Levenberg optimization technique. Different numbers of hidden layer nodes were tried in this study and the condition that gave the minimum difference between predicted and experimental values for the utilization of the validation data set was determined. In the simulations, the stopping criterion was the number of iterations used. Different numbers of iterations were tested to determine the value providing the best results.

A schematic of the GRNN is shown in Fig. 2. The GRNN method does not require an iterative training procedure but instead estimates any arbitrary function between input and output vectors, drawing the function estimate directly from the training data. The GRNN is based on a standard statistical technique called kernel regression [18]. By definition, the regression of a dependent variable  $y$  on an independent  $x$  estimates the most probable value for  $y$ , given  $x$  and a training set. The regression method will produce the estimated value of  $y$ , which minimizes the mean-squared error. The GRNN consists of four layers: input layer, pattern layer, summation layer, and output layer. The first layer is fully connected to the second, pattern layer, where each unit represents a training pattern and its output

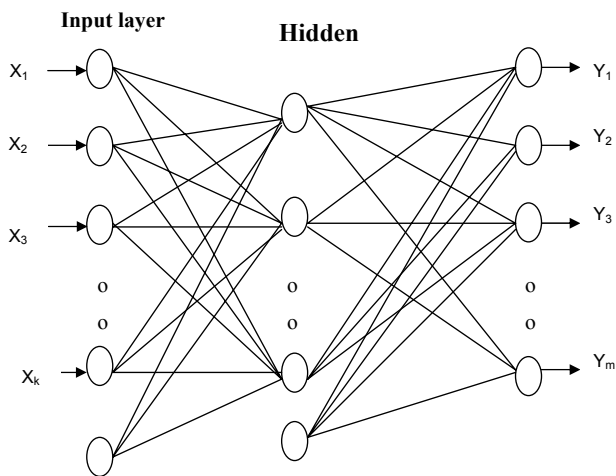


Fig. 1. A schematic of the FFBP neural networks.

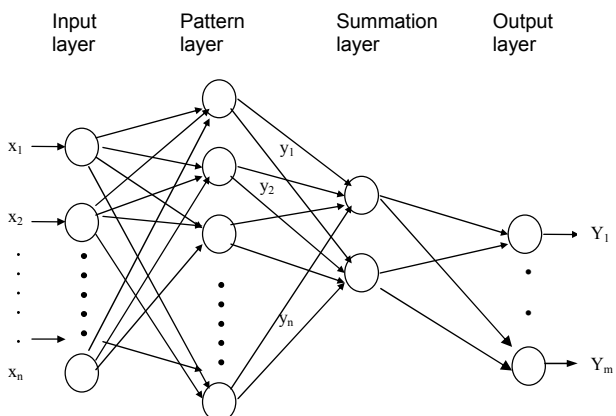


Fig. 2. A schematic of the GRNN.

is a measure of the distance of the input from the stored patterns. Each pattern layer unit is connected to the two neurons in the summation layer: S-summation neuron and D-summation neuron. The S-summation neuron computes the sum of the weighted outputs of the pattern layer while the D-summation neuron calculates the unweighted outputs of the pattern neurons. The connection weight between the  $i^{\text{th}}$  neuron in the pattern layer and the S-summation neuron is  $y_i$ , the target output value corresponding to the  $i^{\text{th}}$  input pattern. For D-summation neuron, the connection weight is unity. The output layer merely divides the output of each S-summation neuron by that of each D-summation neuron. In this method, the spread  $\sigma$  is a smoothing parameter, the optimal value of which is often determined experimentally. In this study, different spreads were tried to find the best one that gave the minimum difference between predicted and experimental values for the utilization of the validation data.

Fig. 3 depicts the structure of RBF neural networks. Radial basis functions are powerful techniques for interpolation in multidimensional space. RBF networks were introduced into the neural network literature as a model motivated by the locally tuned response observed in biological neurons. The theoretical basis of the RBF approach lies in the field of interpolation of multivariate functions [19]. The interpretation of the RBF method as an artificial neural network consists of three layers: a layer of input neurons feeding the feature vectors into the network; a hidden layer of RBF neurons, calculating the outcome of the basis functions; and a layer of output neurons, calculating a linear combination of the basis functions. The input layer sends copies of the input variables to each node in the hidden layer. The nodes in the hidden layer are each specified by a transfer function, which transforms the incoming signals. The network output is given by a linear weighted summation of the hidden node responses at each node in the output layer. In this study, the most common RBF function, i.e. the Gaussian, was employed. Different numbers of hidden layer neurons and spread constants were tried. The hidden layer neuron number that gave the minimum difference between predicted and experimental values for the utilization of the validation data was determined. The spread that gave the minimum relative error was also found simply by a trial-error approach adding some loops on program codes.

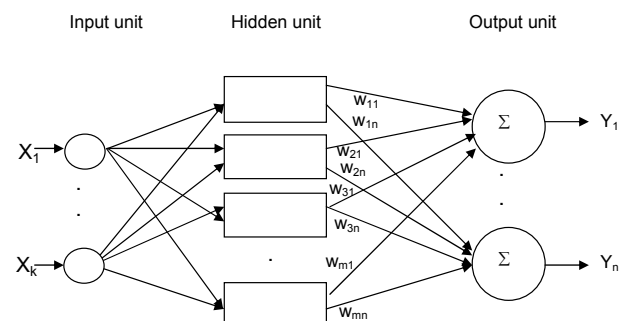


Fig. 3. A schematic of the RBF neural networks.

## Experimental Study

The important characteristics of the fruit juice industry effluents used in this study were:

- (1) high COD concentration
- (2) deficiency in nitrogen and phosphorus
- (3) high acidity with little buffering capacity

Based on filtered samples, the COD of the fruit juice effluent was 80-90%. The characteristics of the citrus juice wastewater and specifications of the full-scale UASB reactor used in this study are listed in Table 1.

Diameter and height of the full-scale reactor were 16 m and 7 m respectively, and it had a total volume of 1,407 m<sup>3</sup>. Constant hydraulic feed to the reactor is important in order to maintain a constant up flow. Constant flow and steady hydraulic conditions further purification was achieved by keeping a recirculation rate of 25-100% according to the influent flow. Temperature in the reactors was maintained at 35°C.

The UASB reactor we used consisted of a main body and the settling zone. All the biological processes took place in the main body filled with sludge that did not contain air. This section was well mixed, owing to the upward flow of the wastewater and the presence of the gas formed during refinement. The settling zone located at the top of the reactor contained a special gas-liquid-solid separator. As the gas bubbles formed in the main body moved upward, some sludge also drifted with them. The gas bubbles, separated from the liquid and solid phases under the funnel, which was placed upside down in the settling zone, left the system through the gas line. In the same while, the freed sludge particles returned to the main body. Similarly, some amount of sludge that drifted by the hydraulic flow inside the reactor settled on the outer side of the funnel and reentered the main body. The feed into the reactor was made from the base. As a result of the mixing of the sludge bed, the wastewater-sludge contact was assured, which increased the wastewater treatment efficiency of the system.

In order to compensate the deficiency of nitrogen and phosphorus in the citrus juice wastewater, NH<sub>4</sub>Cl and K<sub>2</sub>PO<sub>4</sub> were added as nutrients to the wastewater, provided that the COD/N/P ratio was equal to 300/5/1. Additionally, NaHCO<sub>3</sub> was added regularly to provide sufficient alkalinity in the reactor. All the analyses were performed in accordance with Standard Methods [20].

## Method of Estimation

In this study, experimental data pertaining to the UASB reactor operation were utilized in the predictions performed by the FFBP, GRNN, and RBF models. The components of the input vector were flow (m<sup>3</sup>/day), volumetric load (kg/m<sup>3</sup>), and COD<sub>in</sub> (mg/l), as well as TSS<sub>in</sub> (mg/l) concentrations in the influent, while the components of the output vector were COD<sub>out</sub> and TSS<sub>out</sub> concentrations of the effluent as well as biogas production (m<sup>3</sup>/h).

The application of the ANNs to data consisted of two steps. The first step was the training of the neural networks,

Table 1. Characteristics of the citrus juice wastewater and specifications of UASB reactor used in this study.

Component	Value
Chemical oxygen demand, COD <sub>in</sub> (mg/L)	2790-14680
Chemical oxygen demand, COD <sub>out</sub> (mg/L)	20-6690
COD <sub>removal</sub> (%)	16-100
Total Kjeldahl nitrogen, TKN (mg/L)	80-100
Total phosphorus, TP (mg/L)	12-20
Total suspended solids, TSS <sub>in</sub> (mg/L)	150-1750
Total suspended solids, TSS <sub>out</sub> (mg/L)	30-420
Volumetric loading rate (kg COD/m <sup>3</sup> day)	0.9-27.4
Biogas production (m <sup>3</sup> /day)	880-11000
Flow (m <sup>3</sup> /day)	850-1750
Retention time in reactor (h)	28-56
Net sludge production (kg/day)	102-610

including the presentation of training data describing the input and output to the network and obtaining the inter-connection weights. The input and output data were normalized between 0 and 1 prior to training. After the completion of the training stage, the ANNs were applied to the validation data. The network structure providing the best result was determined according to the success of the predictions performed using the validation data set. The ANNs were used to predict only one component of the output vector at a time. Data set 1 (105 data) was used for training the neural networks while data set 2 (8 data) was used for validation. The ranges of values used in the training data were equal to 20-6690 mg/l, 72-2080 mg/l, and 543-14317 m<sup>3</sup>/h for COD<sub>out</sub>, TSS<sub>out</sub>, and biogas production, respectively, while those in the validation data were 1430-2026 mg/l, 140-930 mg/l, and 2078-6489 m<sup>3</sup>/h, respectively, for the same parameters. The validation data were selected in a manner assuring that they remain within the maximum and minimum limits of the training data. It was also observed that when different validation data were utilized, the success of the predictions did not change significantly in this study.

The results obtained by using the FFBP, GRNN, and RBF models were compared to the actual values as well as to the values estimated by using multilinear regression. The regression model utilized in this study was of simple linear form, as given below. R might represent COD<sub>out</sub>, TSS<sub>out</sub>, or biogas production.

$$R = a_0 + a_1(\text{COD}_{in}) + a_2(\text{TSS}_{in}) + a_3(\text{flow}) + a_4(\text{volumetric load}) \quad (1)$$

The coefficients in Eq. (1) were determined by using the Marquardt-Levenberg algorithm.

Table 2. Characteristics of the citrus juice wastewater treated in the UASB reactor.

	First year				Second year			
	Min	Max	Average	Std. Dev.	Min	Max	Average	Std. Dev.
COD <sub>in</sub> (mg/L)	2790	12170	6948	1878	3470	13270	6767	2436
COD <sub>out</sub> (mg/L)	20	6690	1469	1065	227	2640	1428	496
COD <sub>removal</sub> (%)	16	100	79.2	14	57	93	76.9	8.9
Volumetric loading rate (kg COD/m <sup>3</sup> day)	1.8	21.9	8.7	5.2	0.9	9.7	5.7	2.4

The relative error (d) was used to monitor the success of the ANN models and regression used in the prediction of COD<sub>out</sub>, TSS<sub>out</sub>, and biogas production. d was determined by taking into consideration the deviation (%) of these parameters, calculated by using the ANNs or regression (ccalc), from the corresponding actual values (cact).

$$d_m = |c_{act} - c_{calc}| / c_{act} \times 100 \quad (2)$$

...where: d<sub>m</sub> was defined as the arithmetic mean of the relative errors obtained for the different data used in prediction.

## Results and Discussion

### Full-Scale Experiments and UASB Reactor Performance Data

In this study, the full-scale UASB reactor treating citrus juice wastewater was investigated for two years. The citrus juicing season of the food processing plant was typically from November to June and the off-season was from July to November. Figs. 4 and 5 illustrate the variations of the influent and effluent COD concentrations, the related COD

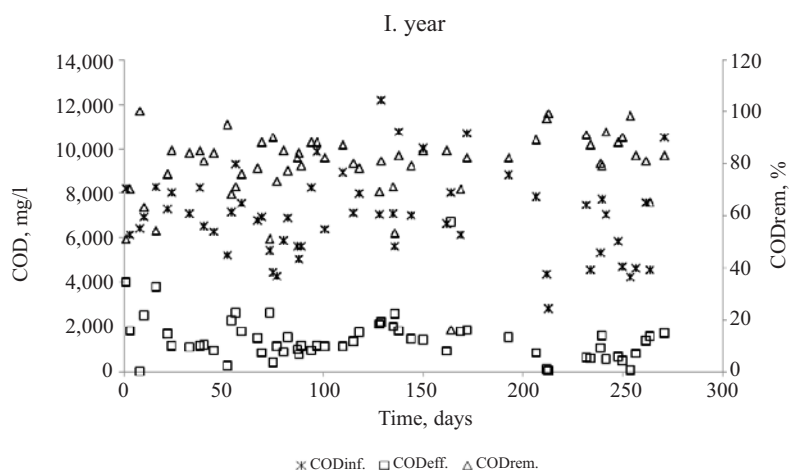


Fig. 4. Influent and effluent COD concentration and related COD removal efficiency in the full-scale reactor during the first year of operation.

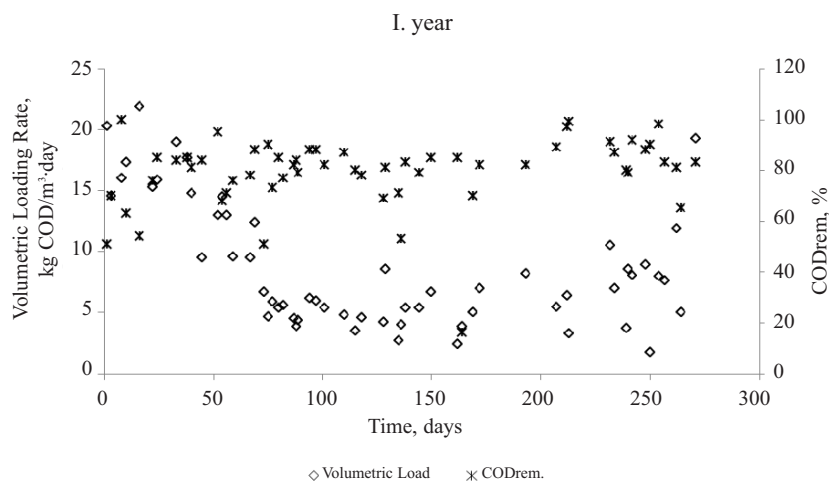


Fig. 5. Volumetric loading rate and related COD removal efficiency in the full-scale reactor during the first year of operation.

removal efficiency performance and the volumetric loading rate of the UASB reactor with time for the first year of operation. Figs. 6 and 7 depict the same variations for the second year of operation. Table 2 summarizes the concentrations of influent and effluent COD and the reactor performance during the two-year period. The reactor was operated for seven months during the first year but only for four months during the second year. It is well known that the start-up period is critical for the anaerobic treatment processes. As seen in the figures, however, the UASB reactor recovered very fast after the off-season for both years. For the first year, COD removal efficiency was over 50% while the volumetric loading rate was as high as 15 kg COD/m<sup>3</sup>day during the start-up period. The COD removal efficiency reached to over 80% in a month. The average removal efficiency and loading rate were 79% and 8.1 kg COD/m<sup>3</sup>day, respectively. For the second year, the loading rates during the working period were lower compared to those in the first year. COD removal efficiency was observed to be equal to 57-93% during the second year. The average removal efficiency was 77% while the average loading rate was 5.7 kg COD/m<sup>3</sup>day.

### Criteria Assuring Best Performance for the ANN Models

The FFBP, GRNN, and RBF models were used to relate COD<sub>out</sub>, TSS<sub>out</sub>, and biogas production to flow, volumetric load, COD<sub>in</sub>, and TSS<sub>in</sub> during the two-year operation of the UASB reactor. The prediction of COD<sub>out</sub>, TSS<sub>out</sub> and biogas production in data set 2 was performed using the three different ANNs mentioned above, and data set 1 for training. As mentioned before, the network structure providing the best result was determined according to the success of the predictions performed using the validation data. It was also established that the conditions providing the best results in the testing stage could allow the ANN methods to exhibit quite high performances in the training stage.

In this study, one hidden layer was found adequate for FFBP simulations. For this method, 150 iterations and 3 hidden layer nodes were the conditions determined to give the best results in both cases. The random weight assignment at the beginning of each training simulation was different. For the GRNN method, spread factors in the range 0.02-0.22 were the conditions determined to give the best results.

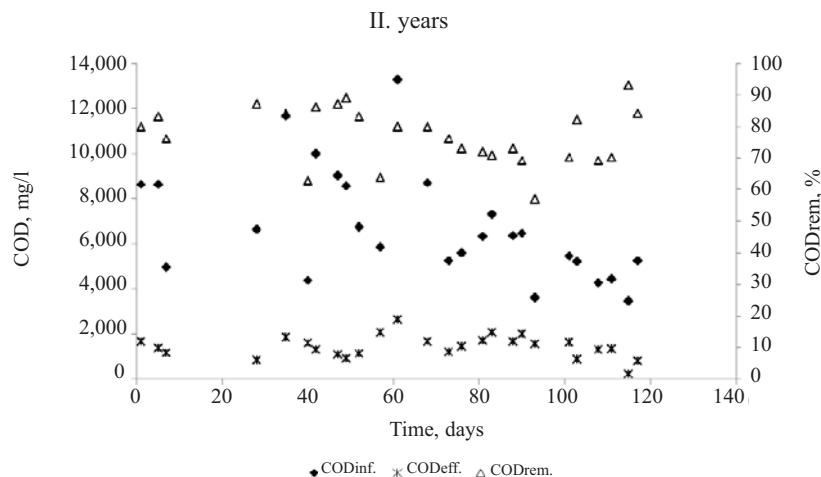


Fig. 6. Influent and effluent COD concentrations and the related COD removal efficiency in the full-scale reactor during the second year of operation.

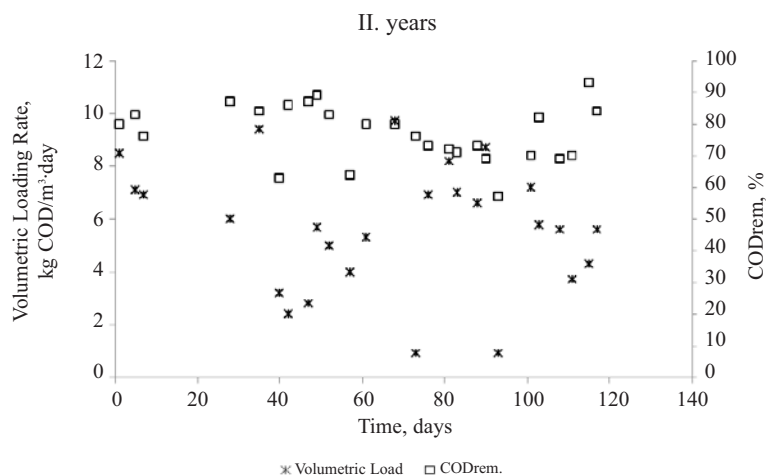


Fig. 7. Volumetric loading rate and related COD removal efficiency in the full-scale reactor during the second year of operation.

Table 3. Average relative errors obtained for the predictions performed using different methods.

Method	d <sub>m</sub> (%)		
	COD <sub>out</sub>	TSS <sub>out</sub>	Biogas production
GRNN	8.9	44.6	12.2
RBF	11.8	46.1	6.7
FFBP	8.9	15.6	6.4
Regression	9.7	67.2	66.0

The spread factor was determined to be equal to 0.22, 0.02, and 0.085 for COD<sub>out</sub>, TSS<sub>out</sub>, and biogas production, respectively, by using validation data set 2 for optimization. The training of the neural networks was carried out by using data set 1. For the RBF method, spreads in the range 0.125-0.565 and 15 neurons were the conditions determined to give the best results. The spread was determined to be equal to 0.125, 0.225 and 0.565 for COD<sub>out</sub>, TSS<sub>out</sub>, and biogas production, respectively, by using the validation data set 2 for optimization. When the optimization was performed using training data, without taking into consideration validation data, the d<sub>m</sub> values, representing the deviation of the predicted values of data set 1 or data set 2 from actual values, were less than 10% for all the cases investigated. When the ANN parameters were optimized using data set 2, the predictive power of the ANN methods was not reduced significantly.

### Evaluation of the Predictions Made by the ANN Methods

The results obtained by the ANNs for the prediction of COD<sub>out</sub>, TSS<sub>out</sub>, and biogas production are depicted in Figs. 8, 9, and 10, respectively. The actual experimental values are also given in the figures. It may be observed from the figures that the ANN methods provided quite good fits in some cases, while they were less successful in some others. The results may be observed more clearly from Table 3, where the average deviation values obtained by using the ANNs from experimental data are presented. The performances exhibited by multilinear regression may also be seen in this table.

In general, the FFBP method was utilized quite successfully to predict the COD<sub>out</sub>, TSS<sub>out</sub>, and biogas production from the experimental training data. This method provided less deviation from the actual experimental values. Additionally, the predictions made for biogas production and COD<sub>out</sub> were more accurate, while relatively larger discrepancies existed for the TSS<sub>out</sub> values. The average relative error in COD<sub>out</sub> prediction, in the best case, was equal to 8.9%, as obtained by using both the GRNN and FFBP methods. For the prediction of TSS<sub>out</sub>, the smallest average relative error (amounting to 15.6%) was obtained by far, by using the FFBP method. The smallest average relative error (6.4% for the prediction of biogas production) also was obtained by the FFBP method.

When multilinear regression was utilized, the average deviation from the actual values was higher than those provided by the ANN models tested with one exception: the prediction of COD<sub>out</sub> by RBF. The average relative error was equal to 9.7, 66.0, and 67.2 for the prediction of COD<sub>out</sub>, TSS<sub>out</sub>, and biogas production, respectively, when

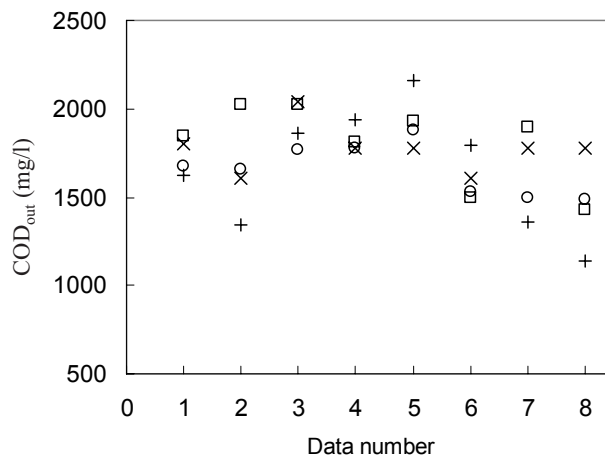


Fig. 8. COD<sub>out</sub> predictions by (o) GRNN, (+) RBF, and (x) FFBP models, in comparison to (□) experimental results.

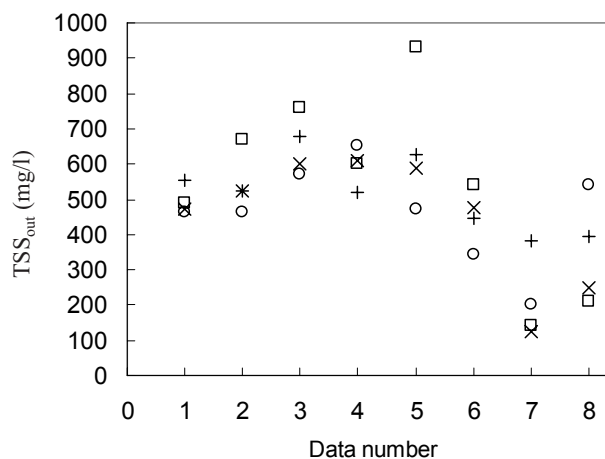


Fig. 9. TSS<sub>out</sub> predictions by (o) GRNN, (+) RBF, and (x) FFBP models, in comparison to (□) experimental results.

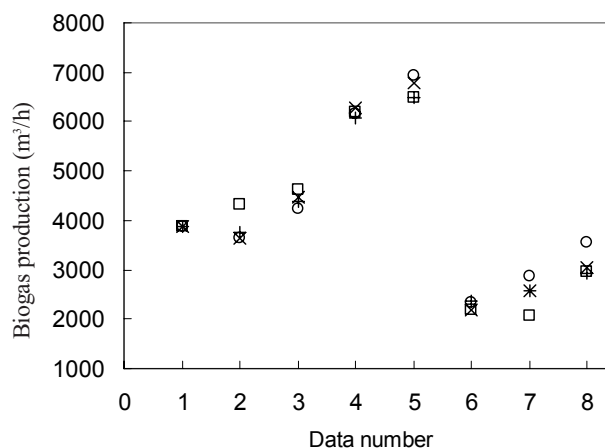


Fig. 10. Biogas production predictions by (o) GRNN, (+) RBF, and (x) FFBP models, in comparison to (□) experimental results.

multilinear regression was utilized. It may be deduced from these results that the best improvement provided by the ANNs over regression was in the prediction of biogas production. The results obtained using multilinear regression and ANNs were the closest in COD<sub>out</sub> prediction.

### Conclusions

Average COD removal efficiencies of about 79% and 77% were obtained during the first and second year of operation, respectively, when a UASB reactor was used in the treatment of citrus juice wastewater. The average volumetric loading rate was equal to 8.1 and 5.7 kg COD/m<sup>3</sup>day, respectively, during these periods of time. It was shown in this study that information might be gained about the significant parameters related to the operation of the USB reactor by using artificial neural network models. The FFBP, GRNN, and RBF models generally provided quite better predictions than multilinear regression for this purpose. The FFBP generally had the highest predictive power for the COD<sub>out</sub>, TSS<sub>out</sub> and biogas production parameters investigated. The best prediction was made for biogas production, which also provided quite a significant improvement over multilinear regression. The few other studies in the literature using neural network models for the modeling of a UASB reactor had also exhibited similar promising results. Especially, the prediction of biogas production rate seems to be closely estimated by these models.

The superiority of the ANNs over conventional methods for the prediction of complex and high dimensional relationships, such as the one investigated in this study, might be attributed to the capability of the ANNs to capture the nonlinear features and generalize the structure of the whole data set.

Artificial neural network methods may be used as a means of modelling the operation of UASB reactors for different conditions. Pattern recognition may be performed to determine unknown output parameters for different reactor input data. In case training data in addition to those adopted in this study are used with ANN models to make the predictions, the relative success of prediction might improve.

### References

1. VAN HAANDEL A.C., LETTINGA G. *Anaerobic Sewage Treatment: A Practical Guide for Region with a Hot Climate*; John Wiley & Sons: New York, **1994**.
2. AIYUK S., FORREZ I., LIEVEN D.K., VAN HAANDEL A., VERSTRAETE W. Anaerobic and complementary treatment of domestic sewage in regions with hot climates - A review. *Biores. Technol.*, **97**, 2225, **2006**.
3. GOMEZ C.Y. High-rate anaerobic treatment of domestic wastewater at ambient operating temperatures: A review on benefits and drawbacks. *J. Environment. Sci. Health Part A*, **45**, 1169, **2010**.
4. LETTINGA G., VANVELSEN A.F.M., HOBMA S.W., DEZEEUW W., KLAPWIJK A. Use of the upflow sludge blanket (USB) reactor concept for biological wastewater treatment, especially for anaerobic treatment. *Biotech. Bioeng.*, **22**, 699, **1980**.
5. KE S., SHI Z. Applications of two-phase anaerobic degradation in industrial wastewater treatment. *Int. J. Environment. Pollut.* **23**, 65, **2005**.
6. VEERESH G.S., KUMAR P., MEHROTRA I. Treatment of phenol and cresols in up-flow anaerobic sludge blanket (UASB) process: a review. *Water Research* **39**, 154, **2005**.
7. DEMIREL B., YENIGUN O., ONAY T.T. Anaerobic treatment of dairy wastewaters: a review. *Process Biochem.* **40**, 2583, **2005**.
8. ERGUDER T.H., TEZEL U., GUVEN E., DEMIRER, G.N. Anaerobic biotransformation and methane generation potential of cheese whey in batch and UASB reactors. *Waste Manag.* **21**, 643, **2001**.
9. KALYUZHNYI S., FEDOROVICH V. Integrated mathematical model of UASB reactor for competition between sulphate reduction and methanogenesis. *Water Sci. Technol.* **36**, 201, **1997**.
10. BARAMPOUTI E.M.P., MAI S.T., VLYSSIDES A.G. Dynamic modeling of biogas production in an UASB reactor for potato processing wastewater treatment. *Chem. Eng. J.* **106**, 53, **2005**.
11. BHUNIA P., GHANGREKAR M.M. Statistical modeling and optimization of biomass granulation and COD removal in UASB reactors treating low strength wastewaters. *Bioresource Technol.* **99**, 4229, **2008**.
12. VLYSSIDES A., BARAMPOUTI E.M., MAI S. An alternative approach of UASB modeling. *AIChE J.* **53**, 3269, **2007**.
13. SINGH K.P., BASANT N., MALIK A., JAIN G. Modeling the performance of "up-flow anaerobic sludge blanket" reactor based wastewater treatment plant using linear and nonlinear approaches-A case study. *Analyt. Chim. Acta*, **658**, 1, **2010**.
14. SINHA S., BOSE P., JAWED M., JOHN S., TARE V. Application of neural network for simulation of up-flow anaerobic sludge blanket (UASB) reactor performance. *Biotechnol. Bioeng.* **77**, 806, **2002**.
15. MU Y., YU H.Q. Simulation of biological hydrogen production in a UASB reactor using neural network and genetic algorithm. *Int. J. Hydrogen Energ.* **32**, 3308, **2007**.
16. KANAT G., SARAL A. Estimation of biogas production rate in a thermophilic UASB reactor using artificial neural networks. *Environ. Model. Assess.* **14**, 607, **2009**.
17. HAGAN M.T., MENHAJ M.B. Training feed forward networks with the Marquardt algorithm. *IEEE Trans. Neural Networks* **6**, 861, **1994**.
18. KIM B., KIM S., KIM K. Modeling of plasma etching using a generalized regression neural network. *Vacuum* **71**, 497, **2003**.
19. TAURINO A.M., DISTANTE C., SICILIANO P., VASANELLI L. Quantitative and qualitative analysis of VOCs mixtures by means of a microsensor array and different evaluation methods. *Sens. Act.* **93**, 117, **2003**.
20. APHA-AWWA-WPCF Standard methods for the examination of water and wastewater, 20<sup>th</sup> edition: Washington, DC, **1998**.